Available online at www.sciencedirect.com
ScienceDirect
Signal Processing 87 (2007) 220–236
SIGNAL PROCESSING
www.elsevier.com/locate/sigpro

Spectral decomposition of a 4th-order covariance tensor: Applications to diffusion tensor MRI

Peter J. Basser[a,*], Sinisa Pajevic[b]

[a]Section on Tissue Biophysics and Biomimetics, LIMB, NICHD, NIH, Bldg. 13, Rm., 3W16, 13 South Drive, Bethesda, MD 20892, USA
[b]Mathematical and Statistical Computing Laboratory, CIT, NIH, Bethesda, MD 20892-5772, USA

Received 2 August 2005; accepted 27 February 2006
Available online 27 June 2006

Abstract

We propose a novel spectral decomposition of a 4th-order covariance tensor, Σ. Just as the variability of vector (i.e., a 1st-order tensor)-valued random variable is characterized by a covariance matrix (i.e., a 2nd-order tensor), S, the variability of a 2nd-order tensor-valued random variable, D, is characterized by a 4th-order covariance tensor, Σ. Accordingly, just as the spectral decomposition of S is a linear combination of its eigenvalues and the outer product of its corresponding (1st-order tensors) eigenvectors, the spectral decomposition of Σ is a linear combination of its eigenvalues and the outer product of its corresponding 2nd-order eigen*tensors*. Analogously, these eigenvalues and 2nd-order eigentensors can be used as features with which to represent and visualize variability in tensor-valued data. Here we suggest a framework to visualize the angular structure of Σ, and then use it to assess and characterize the variability of synthetic diffusion tensor magnetic resonance imaging (DTI) data. The spectral decomposition suggests a hierarchy of symmetries with which to classify the statistical anisotropy inherent in tensor data. We also present maximum likelihood estimates of the sample mean and covariance tensors associated with D, and derive formulae for the expected value of the mean and variance of the projection of D along a particular direction (i.e., the apparent diffusion coefficient or *ADC*). These findings would be difficult, if not impossible, to glean if we treated 2nd-order tensor random variables as vector-valued random variables, which is conventionally done in multi-variate statistical analysis.

Keywords: PCA; Covariance; Tensor; HOS; Multi-linear algebra; DTI; DT-MRI; Karhunen-Loéve; Anisotropy

1. Introduction

Methods to characterize the variability of scalar and vector-valued random variables are well established. Sample covariance matrices can be analyzed using a variety of methods, such as Principal Component Analysis (PCA) (originally proposed by Pearson [1], and developed by Hotelling [2]), Factor Analysis [3], and Independent Component Analysis (ICA) [4–7]. However, how does one characterize the variability of a *tensor*-valued random variable? Presently, no analogous statistical analysis framework exists [8]. Yet, tensor-valued random variables are ubiquitous in the physical and

*Corresponding author. Tel.: +1 301 435 1949; fax: +1 301 435 5035.
E-mail address: pjbasser@helix.nih.gov (P.J. Basser).

0165-1684/$ - see front matter © 2006 Elsevier B.V. All rights reserved.
doi:10.1016/j.sigpro.2006.02.050

Nomenclature

x	normal random vector, i.e., N-dimensional 1st-order tensor
M	2nd-order symmetric covariance matrix ($N \times N$)
D	3-D, 2nd-order symmetric tensor random variable
Σ	3-D, 4th-order covariance tensor ($3 \times 3 \times 3 \times 3$)
S	3-D, equivalent 2nd-order covariance tensor (6×6)
$x^{\mathrm{T}}S^{-1}x$	quadratic function of elements of x, i.e., 0th-order tensor
$D{:}\Sigma^{-1}{:}D$	quadratic function of elements of D, i.e., 0th-order tensor
$p(x)$	normal multi-variate pdf of x
$p(D)$	normal tensor-variate pdf of D
$\bar{D}$	mean tensor of D
$\tilde{D}$	2nd-order symmetric tensor random variable written as a 6×1 vector
$L(p(D))$	likelihood function of $p(D)$
$\delta_{ij}^{\ 3}$	Kronecker delta or 3-dimensional identity matrix (3×3)
$\delta_{ij}^{\ 6}$	Kronecker delta or 6-dimensional identity matrix (6×6)
σ_k	kth Eigenvalue of Σ or S
ε_i^k	kth Eigenvector of S (6×1)
E^k	kth 2nd-order Eigentensor of Σ (3×3)
γ_i^k	ith Eigenvalue of E^k
v_i^k	ith Eigenvector of E^k (3×1)
λ_j	jth Eigenvalue of D
η_j	jth Eigenvector of D (3×1)
$\hat{r}$	unit radial direction vector
$\mathbf{r}$	3-D position vector

imaging sciences. For instance, in diffusion tensor magnetic resonance imaging (DTI or DT-MRI), a symmetric 2nd-order diffusion tensor is statistically estimated in each voxel within an imaging volume [9,10].

Specifically, we would like to extract useful features that describe the variability of the estimated diffusion tensor in each voxel within an imaging volume. In particular, we would like to segment regions of interest (ROIs) in which diffusion properties are similar, and ultimately compare their features to those in other ROIs in the same subject (e.g., in a longitudinal study) or in different subjects (e.g., in a multi-site study). Efforts to advance these activities have been stymied by the dearth of adequate statistical analysis methods to describe the inherent variability of tensor and tensor field data.

To address these limitations, we propose a framework to characterize the covariance structure of random 2nd-order tensor variables. We present expressions for the sample mean and covariance *tensors* associated with a 2nd-order tensor random variable, and show that the covariance tensor is a positive definite 4th-order tensor, which can be decomposed as a linear combination of eigenvalues and the outer product of their corresponding eigen*tensors*. We suggest how to classify this 4th-order covariance tensor according to its symmetry properties and its distinct spectral features. We also propose a new way to visualize angular or orientational features of the 4th-order covariance tensor using the spectral decomposition framework.

An interesting application of this framework is to analyze DTI data. Using Monte Carlo methods, we generate ideal DTI data (with Johnson or thermal background noise added) assuming properties of neural tissue found in human brain.

2. Background

The variability and common features embedded within vector-valued data or image arrays are often extracted using a spectral expansion, often referred to as a Karhunen-Loéve decomposition, which determines distinct "modes" in random signals. In PCA, one identifies and retains the dominant modes by truncating this series. In this work, we primarily focus on obtaining and analyzing the entire spectral expansion; we ignore the issue of data reduction or compression, but these also can be addressed using the methodology we present below.

To perform a spectral analysis on vector-valued data, one first obtains a (sample) covariance matrix, S, and then expands it as a linear combination of eigenvalues and the outer product of their

corresponding eigenvectors (e.g., see [11]). There are, however, many data types, such as 2nd- and higher order tensors, for which this approach is problematic. Although it is always possible to write these tensors as vectors (e.g., see [12,13]), repacking tensor elements in this way obscures certain intrinsic algebraic relationships among them (e.g., failing to distinguish between diagonal and off-diagonal tensor elements). Specifically, while it is straightforward to expand a 2nd-order tensor in its "native" form in terms of its eigenvalues and eigenvectors, or to apply to it an affine transformation (e.g., rotation, dilation, or shear), these operations are unwieldy when the tensor is written as a vector [14]. Representing 2nd-order tensors as vectors also obscures their intrinsic geometric structure. For example, while we can readily represent quadratic forms associated with 2nd-order symmetric tensors graphically as 3-dimensional ellipsoids, paraboloids, or hyperboloids, we lose this ability to represent geometric features when writing these tensors as 6-dimensional vectors. By preserving the form of a tensor random variable, we retain our ability to perform algebraic operations and interpret their underlying intrinsic geometric structure.

A case in point is DTI. It was previously shown that a normal multi-variate distribution could describe the distribution of a 2nd-order diffusion tensor (measured in the laboratory coordinate system) if one rewrites this tensor as a 6-dimensional vector [15]. This distribution allowed us to characterize the uncertainty and correlation among tensor elements, and even predict the distribution of an important tensor-derived quantity, Trace(D) [16]. However, using this vector form, one cannot easily assess how rotating the laboratory coordinate system affects the distribution of these tensor elements or even determine the variability of the projection of this tensor along a particular direction (i.e., the apparent diffusion coefficient or ADC). Moreover, writing the 2nd-order diffusion tensor as a vector also complicates attempts to obtain a distribution of other tensor-derived quantities, such as its eigenvalues and eigenvectors [17].

These considerations led us to propose a normal distribution for 2nd-order (and higher order) tensor data [17], which generalizes the normal multi-variate distribution. In order to preserve the form of the tensor random variable in this new distribution, we replaced the familiar mean vector, μ, in the multi-variate normal distribution, with a 3-dimensional 2nd-order mean tensor, $\bar{D}$, and replaced the covariance matrix, S, in the multi-variate normal distribution, with a 3-dimensional 4th-order covariance tensor, Σ. However, in considering the properties of this new distribution, and in particular, in extracting useful features from Σ, we were led to examine the spectral expansion of Σ, i.e., a decomposition of Σ into a linear combination of eigenvalues and eigen*tensors*. We will see that this spectral decomposition yields insights into the behavior of 2nd-order tensor random variables, producing a myriad of new features with which to classify and cluster tensor data, and a means to visualize these features in 3-dimensions.

3. Theory

3.1. The normal distribution for 2nd-order tensor random variables

Recall that the exponent of a multi-variate normal probability density function, $p(x)$, contains the quadratic form, $(x-\mu)^{\mathrm{T}}M^{-1}(x-\mu)$, of an N-dimensional normal random vector, x, its mean vector, μ, and the inverse of an $N\times N$ covariance matrix, M [18,19]:

$$p(x) = \sqrt{\frac{|M^{-1}|}{(2\pi)^N}}\,\mathrm{e}^{-(1/2)(x-\mu)^{\mathrm{T}}M^{-1}(x-\mu)} = \sqrt{\frac{|M^{-1}|}{(2\pi)^N}}\,\mathrm{e}^{-(1/2)(x_i-\mu_i)^{\mathrm{T}}M_{ij}^{-1}(x_j-\mu_j)}, \quad (1)$$

where we use the Einstein summation convention in the second expression above. The exponent $(x_i-\mu_i)^{\mathrm{T}}M_{ij}^{-1}(x_j-\mu_j)$ is a scalar contraction of two N-dimensional 1st-order tensors, $x_i-\mu_i$ and $x_j-\mu_j$ and the inverse of the N-dimensional 2nd-order covariance tensor,[1] M_{ij}. Using either convention, the exponent is a sum of quadratic functions containing products of components of $x-\mu$ weighted by the respective elements of M^{-1}.

However, the interpretation of the random vector and covariance matrix as tensors of 1st- and 2nd-order, respectively, suggests how to generalize the multi-variate normal distribution to *tensor*-variate normal distribution for a 2nd-order random

[1] In this context, S is usually referred to as a matrix, but it transforms as an N-dimensional 2nd-order tensor.

tensor, D,[2]

$$p(D) = \sqrt{\frac{|\Sigma^{-1}|}{8\pi^6}}\, e^{-(1/2)(D-\bar{D}):\Sigma^{-1}:(D-\bar{D})} = \sqrt{\frac{|\Sigma^{-1}|}{8\pi^6}}\, e^{-(1/2)(D_{ij}-\bar{D}_{ij}):\Sigma^{-1}_{ijmn}:(D_{mn}-\bar{D}_{mn})}. \quad (2)$$

Above, $\bar{D}$ is the mean tensor, and $(D_{ij}-\bar{D}_{ij}):\Sigma^{-1}_{ijmn}:(D_{mn}-\bar{D}_{mn})$ is a scalar contraction[3] of the inverse of the 3-dimensional 4th-order covariance tensor, Σ_{ijkl}, and two 3-dimensional 2nd-order tensors, $(D_{ij}-\bar{D}_{ij})$ and $(D_{mn}-\bar{D}_{mn})$ [17]. Analogously, the resulting exponent is a linear combination of quadratic functions formed from products of elements of D, $(D_{ij}-\bar{D}_{ij})(D_{mn}-\bar{D}_{mn})$, weighted by the appropriate coefficients, Σ^{-1}_{ijmn}.

A few points need to be made to clarify the meaning of Eq. (2). First, we use the tensor "double dot product" operator above in Eq. (2) as defined in [20]. Formally, in the expression $D:\Sigma^{-1}:D = D_{ij}\Sigma^{-1}_{ijkl}D_{kl}$, sums are taken over all values of the four indices, i, j, k, and l. The meaning of the inverse 4th-order tensor, Σ^{-1}, also merits some explanation. Σ and Σ^{-1} are both 4th-order tensors related to the symmetric 4th-order identity tensor, Y, by

$$\Sigma_{ijkl}\Sigma^{-1}_{klmn} = \Sigma^{-1}_{ijkl}\Sigma_{klmn} = Y_{ijmn} = \frac{1}{2}(\delta_{im}\delta_{jn} + \delta_{in}\delta_{jm}). \quad (3)$$

Finally, the definition of the determinant of the 4th-order tensor, $|\Sigma^{-1}|$, appearing in Eq. (2), is given below in Eq. (13), and will be used below to explain the differences in normalization constants appearing in Eqs. (1) and (2).

3.2. Symmetry properties of the 4th-order covariance tensor, Σ

When D is a symmetric 2nd-order tensor, Σ will inherit symmetries such that certain elements are unaltered by the exchange of particular pairs of indices of D. For simplicity, we will set the mean tensor, $\bar{D}$, to zero for now. Since the product of two elements of the 2nd-order tensor commute in the scalar contraction, $D_{ij}\Sigma^{-1}_{ijmn}D_{mn}$, i.e., $D_{ij}D_{mn} = D_{mn}D_{ij}$, the corresponding coefficients of Σ are indistinguishable and must be the same, i.e., $\Sigma_{ijmn} = \Sigma_{mnij}$. In addition, since D is symmetric, i.e., $D_{ij} = D_{ji}$ and $D_{mn} = D_{nm}$, we require that $\Sigma_{ijmn} = \Sigma_{jimn}$ and $\Sigma_{ijmn} = \Sigma_{ijnm}$, respectively. These symmetries, which are well-known in the continuum mechanics literature, reduce the possible number of independent elements required to specify Σ from 81 (i.e., 3^4) to 21 [21].

In fact, we can adopt the schema used to classify symmetries in 4th-order elasticity tensors appearing in the theory of continuous media (e.g., [22]) for this statistical application. The general linear elastic model, *aelotropic* or *triclinic,* requires specifying all 21 independent constants [23]. Other models require fewer independent constants (e.g., see [23]). These include the cases of *planar symmetric* or *monoclinic*, requiring 13 coefficients; *orthotropic*, requiring 9 coefficients; *transverse isotropic*, requiring 5 coefficients; *cubic orthotropy*, requiring 3 coefficients [24]; and *isotropic*, requiring only 2 coefficients.[4] See Sutcliffe [25] for examples of different materials whose 4th-order elasticity tensors exhibit these various symmetry conditions.

It is not a coincidence that 21 independent elements are also required to specify each element of the symmetric covariance matrix, S. In fact, any 3-dimensional 4th-order tensor, Σ, satisfying the symmetry properties given above, can be mapped to a 6-dimensional 2nd-order tensor, S, (represented as a symmetric 6×6 matrix), containing the same 21 independent coefficients (e.g., see [13,23,26]).

To do this, we first note that the scalar contraction, $D_{ij}\Sigma^{-1}_{ijmn}D_{mn}$, above can also be written as a quadratic form, $\tilde{D}_r S^{-1}_{rt}\tilde{D}_t$, in which the random 2nd-order tensor, D_{ij}, is written as a 6-dimensional column vector, $\tilde{D}$, where $\tilde{D} = (D_{xx}, D_{yy}, D_{zz}, \sqrt{2}D_{xy}, \sqrt{2}D_{xz}, \sqrt{2}D_{yz})^{\mathrm{T}}$. The factors of $\sqrt{2}$ premultiplying the off-diagonal elements of D_{ij} ensure that the matrix multiplication operation between $\tilde{D}$ and the 6-dimensional 2nd-order tensor, S, is isomorphic to the tensor double dot product operation between the 2nd-order tensor D, and the 3-dimensional 4th-order tensor, Σ. More about this issue can be found in [27,28].

To convert between the 6-dimensional 2nd-order covariance tensor and the 3-dimensional 4th-order

[2]N.B. The tensors we consider here are Cartesian, so that it is not necessary to distinguish between covariant and contravariant indices.

[3]N.B. The contraction appearing in the exponent of Eq. (2) should be unitless. Therefore, whatever physical units the 2nd-order tensor may possess, the 4th-order covariance must be the square of this. So, if one measures D in dimensions of length^2/time (L^2/T), then for consistency, the dimensions of Σ would be L^4/T^2.

[4]Hexagonal and tetragonal cases, each requiring 6 or 7 independent parameters, can also be considered.

covariance tensor representations, we use

$$S = \begin{pmatrix} \Sigma_{xxxx} & \Sigma_{xxyy} & \Sigma_{xxzz} & \sqrt{2}\Sigma_{xxyy} & \sqrt{2}\Sigma_{xxxz} & \sqrt{2}\Sigma_{xxyz} \\ \Sigma_{xxyy} & \Sigma_{yyyy} & \Sigma_{yyzz} & \sqrt{2}\Sigma_{yyxy} & \sqrt{2}\Sigma_{yyxz} & \sqrt{2}\Sigma_{yyyz} \\ \Sigma_{xxzz} & \Sigma_{yyzz} & \Sigma_{zzzz} & \sqrt{2}\Sigma_{zzxy} & \sqrt{2}\Sigma_{zzxz} & \sqrt{2}\Sigma_{zzyz} \\ \sqrt{2}\Sigma_{xxxy} & \sqrt{2}\Sigma_{yyxy} & \sqrt{2}\Sigma_{zzxy} & 2\Sigma_{xyxy} & 2\Sigma_{xyxz} & 2\Sigma_{xyyz} \\ \sqrt{2}\Sigma_{xxxz} & \sqrt{2}\Sigma_{yyxz} & \sqrt{2}\Sigma_{zzxz} & 2\Sigma_{xyxz} & 2\Sigma_{xzxz} & 2\Sigma_{xzyz} \\ \sqrt{2}\Sigma_{xxyz} & \sqrt{2}\Sigma_{yyyz} & \sqrt{2}\Sigma_{zzyz} & 2\Sigma_{xyyz} & 2\Sigma_{xzyz} & 2\Sigma_{yzyz} \end{pmatrix}. \tag{4}$$

Again, factors of 2 and $\sqrt{2}$ premultiplying different 3×3 "blocks" of the S matrix ensure that this object transforms as a 6-dimensional 2nd-order tensor (see [29,30]) and that the mapping between Σ and S and the corresponding multiplication operations is an isomorphism. In other words, the set of 4th-order symmetric covariance tensors, with the column operation, ":", is isomorphic to the set of 2nd-order covariance tensors and the matrix multiplication operation. In this way, the inverse of the 4th-order tensor can be obtained from S^{-1}, which exists since S in Eq. (4) is symmetric and positive definite.

3.3. Determining the eigenvalues and eigentensors of Σ

Just as one can determine the eigenvalues and eigenvectors of a 2nd-order tensor, one can determine the eigenvalues, σ^2, and 2nd-order eigentensors, E, of a 4th-order tensor [20,24,31]. The fundamental equation is given below [12]:

$$\Sigma : E = \sigma^2 E, \tag{5}$$

where we have used the tensor double dot product "**:**" to signify the tensor product operator.[5] Regrouping terms we obtain

$$(\Sigma - \sigma^2 Y) : E = 0, \tag{6}$$

where Y is a 4th-order identity tensor defined in Eq. (3) above. Just as with square matrices, this equation has a "non-trivial" solution for E if and only if:

$$|\Sigma - \sigma^2 Y| = 0. \tag{7}$$

The six roots of the characteristic equation for σ_i^2 are the six eigenvalues of Σ associated with the six eigentensors, E^i, which form an orthogonal basis for Σ.

Practically, we perform this spectral (or eigentensor) decomposition by exploiting the correspondence between the 4th-order tensor, Σ, and the 6×6 matrix, S, as in Eq. (4) [12]. First, we find the eigenvalues and eigenvectors of S in Eq. (4). The eigenvalues of Σ and S are the same. We construct the 2nd-order eigentensors of Σ from the 6×1 eigenvectors of S, using the following assignment:

$$E^i = \begin{pmatrix} \varepsilon^i_{xx} & \frac{1}{\sqrt{2}}\varepsilon^i_{xy} & \frac{1}{\sqrt{2}}\varepsilon^i_{xz} \\ \frac{1}{\sqrt{2}}\varepsilon^i_{xy} & \varepsilon^i_{yy} & \frac{1}{\sqrt{2}}\varepsilon^i_{yz} \\ \frac{1}{\sqrt{2}}\varepsilon^i_{xz} & \frac{1}{\sqrt{2}}\varepsilon^i_{yz} & \varepsilon^i_{zz} \end{pmatrix}, \tag{8}$$

where $\varepsilon^i = (\varepsilon^i_{xx}, \varepsilon^i_{yy}, \varepsilon^i_{zz}, \varepsilon^i_{xy}, \varepsilon^i_{xz}, \varepsilon^i_{yz})^{\mathrm{T}}$ is the ith normalized eigenvector of S.

The six 3×3 eigentensors, E^i, are symmetric and mutually orthogonal, satisfying

$$E^i : E^j = \delta^3_{ij}, \tag{9}$$

where ${\delta_{ij}}^3$ is the familiar Kronecker delta or 3-dimensional 2nd-order identity tensor. This expression is equivalent to the orthonormality condition for the six 6×1 eigenvectors of the corresponding covariance matrix, S:

$$\varepsilon^i \cdot \varepsilon^j = \delta^6_{ij} \tag{10}$$

where ${\delta_{ij}}^6$ is the Kronecker delta or 6-dimensional 2nd-order identity tensor.[6]

[5] In the case of tensors of the same order, S and T, the tensor dot product is given by

$$S : T = \mathrm{Trace}(ST^{\mathrm{T}}) = S_{ij}T_{kj}\delta_{ik} = S_{ij}T_{ij}.$$

This expression also reduces to the familiar vector dot product, "$\cdot$" for tensors of order one since $\mathrm{Trace}(S\ T^{\mathrm{T}}) = \mathrm{Trace}(T^{\mathrm{T}}\ S) = T \cdot S$.

[6] The superscripts appearing on the Kronecker delta, δ^6_{ij} and δ^3_{ij}, are not standard but are used as an aid to the reader to distinguish between the 3-dimensional and 6-dimensional 2nd-order tensors.

3.4. The spectral decomposition of Σ

It is possible to decompose the 4th-order positive definite symmetric tensor, Σ, into a linear combination of six positive eigenvalues, σ_k^2, multiplied by the outer product of their respective six 2nd-order eigentensors, $E^k \otimes E^k$, i.e.,

$$\Sigma_{ijmn} = \sigma_k E^k_{ij} E^k_{mn} \sigma_k \quad \text{or} \quad \Sigma = \sigma_k E^k \otimes E^k \sigma_k, \tag{11}$$

which we refer to as the spectral decomposition of a 4th-order covariance tensor. Interestingly, the mathematical underpinnings of this spectral decomposition are due to Lord Kelvin [24,31] who used it originally to identify normal mechanical modes of deformations of linearly elastic media, and to classify various material symmetries in anisotropic media.

Σ is positive definite, possessing six positive real eigenvalues (although some may be degenerate (i.e., may repeat (see [13]))), and six corresponding real-valued 2nd-order eigen*tensors*.

The formula above also provides a convenient method for calculating the inverse of the covariance tensor, Σ^{-1}_{ijmn}, found in Eq. (2):

$$\Sigma^{-1}_{ijmn} = \sigma_k^{-1} E^k_{ij} E^k_{mn} \sigma_k^{-1} \quad \text{or} \quad \Sigma^{-1} = \sigma_k^{-1} E^k \otimes E^k \sigma_k^{-1}, \tag{12}$$

which we have previously called the 4th-order *precision* tensor, A [17]. A clear and concise summary of this eigentensor decomposition can also be found in [30].

Moreover, this tensor decomposition provides a simple expression for the determinant of the 4th-order tensor, $|\Sigma|$, i.e.,

$$|\Sigma| = \prod_{k=1}^{6} \sigma_k^2 \quad \text{and} \quad |\Sigma^{-1}| = \prod_{k=1}^{6} \sigma_k^{-2}, \tag{13}$$

which can be used in computing the normalization constant in Eq. (2) above, and explain the multiplicative factor of $2^{3/2}$ between the normalization constants in Eqs. (1) and (2). This factor is simply the ratio of determinants of $|M|$ in Eq. (1) and $|\Sigma| = |S|$ in Eq. (2) or, equivalently, is the Jacobian of the transformation between $\tilde{D}$ and D.

3.5. The spectral decomposition when Σ is an isotropic 4th-order tensor

A particularly interesting special case is one in which Σ is an isotropic 4th-order tensor, Σ^{iso}. This guarantees that Σ has no orientation dependence, making it important in optimal experimental design where one would like to eliminate any orientational sampling or estimation bias [17]. When D is a symmetric 2nd-order tensor, Σ^{iso} must have the form (e.g., see [21,26,30])[7]

$$\Sigma^{\text{iso}}_{ijkl} = \frac{\chi_\kappa}{3}\,\delta_{ij}\delta_{kl} + \chi_\mu\left(\frac{1}{2}(\delta_{ik}\delta_{jl} + \delta_{il}\delta_{jk}) - \frac{1}{3}\,\delta_{ij}\delta_{kl}\right), \tag{14}$$

where χ_κ and χ_μ are constants that, in classical elasticity theory, are related to the bulk and shear moduli [22].

The spectral decomposition of Σ^{iso} has the following eigenvalues:

$$\sigma_1^2 = \chi_\kappa; \quad \sigma_2^2 = \sigma_3^2 = \sigma_4^2 = \sigma_5^2 = \sigma_6^2 = \chi_\mu \tag{15a}$$

and their corresponding normalized eigentensors are

$$E^1 = \tfrac{1}{\sqrt{3}}\begin{pmatrix} 1 & 0 & 0 \\ 0 & 1 & 0 \\ 0 & 0 & 1 \end{pmatrix}, \quad E^2 = \tfrac{1}{\sqrt{6}}\begin{pmatrix} 1 & 0 & 0 \\ 0 & -2 & 0 \\ 0 & 0 & 1 \end{pmatrix},$$
$$E^3 = \tfrac{1}{\sqrt{2}}\begin{pmatrix} 1 & 0 & 0 \\ 0 & 0 & 0 \\ 0 & 0 & -1 \end{pmatrix}, \quad E^4 = \tfrac{1}{\sqrt{2}}\begin{pmatrix} 0 & 1 & 0 \\ 1 & 0 & 0 \\ 0 & 0 & 0 \end{pmatrix},$$
$$E^5 = \tfrac{1}{\sqrt{2}}\begin{pmatrix} 0 & 0 & 1 \\ 0 & 0 & 0 \\ 1 & 0 & 0 \end{pmatrix}, \quad E^6 = \tfrac{1}{\sqrt{2}}\begin{pmatrix} 0 & 0 & 0 \\ 0 & 0 & 1 \\ 0 & 1 & 0 \end{pmatrix}. \tag{15b}$$

In applied mechanics, these eigentensors are principal strain tensors that correspond to distinct modes of deformation. Eigentensor E^1 corresponds to pure dilatation (i.e., volumetric expansion or reduction) with no shape change, whereas all other eigenmodes are iso-volumic (i.e., because $\text{Trace}(E) = 0$) but result in a shape change. E^2 can be produced by a two-unit compressive strain along y and unit extensional strains along x and z, whereas E^3 is produced by a unit compressive strain along z, a unit extensional strain along x, and zero strain along y. E^4, E^5, and E^6 all correspond to pure shear deformations: E^4 corresponds to pure shear strain parallel to the x–y plane, E^5 corresponds to pure shear strain parallel to the x–z plane, and E^6 corresponds to pure shear strain parallel to the y–z

[7] Generally, there is a third term appearing in the expression for an isotropic 4th-order tensor, which contains an anti-symmetric tensor, but this term can be safely ignored when D is a symmetric 2nd-order tensor.

plane. While the statistical interpretation of these "modes" of Σ^{iso} is less concrete, they nonetheless epitomize distinct paradigmatic classes or types of coupling between and/or among different elements of the 2nd-order tensor random variable, D.

Note that the symmetric eigentensors in Eq. (15b) are not generally full Rank or even positive definite. In fact, only E^1 is Rank 3 and positive definite. With the exception of E^1, none of the other eigentensors of Σ^{iso} could be interpretable as a proper diffusion tensor.[8]

It is worth noting that the cubic orthotropy tensor, a, which is described by only three parameters, a, b, and c, such that in the principal coordinate frame, $\Sigma_{xxxx} = \Sigma_{yyyy} = \Sigma_{zzzz} = a$, $\Sigma_{xxyy} = \Sigma_{xxyy} = \Sigma_{yyzz} = b$, $\Sigma_{xyxy} = \Sigma_{xzxz} = \Sigma_{yzyz} = c$, shares the same eigentensors as the isotropic tensor (Eq. (15b)). However, the eigenvalues of the isotropic tensor have a 5-fold degeneracy (Eq. (15a)), while the eigenvalues of the cubic orthotropic tensor have 2-fold and 3-fold degeneracy. This renders the cubic orthotropy tensor rotationally variant.

3.6. Scalar Invariants of Σ

The six coefficients of the 6th-order characteristic equation above in Eq. (7) are each scalar invariants of Σ. In principle, these (or functions of them) can be used as a set of coordinate-free quantities with which to segment or classify different statistical "modes" that one observes.

The simplest way to obtain these invariants, I_1 through I_6, is by expanding the characteristic equation (Eq. (7)) wherein $(\beta) = (\sigma)^2$:

$$(\beta - \sigma_1^2)(\beta - \sigma_2^2)(\beta - \sigma_3^2)(\beta - \sigma_4^2)\\ (\beta - \sigma_5^2)(\beta - \sigma_6^2) = 0, \tag{16}$$

collecting the coefficients with like powers of σ, and writing these coefficients in terms of the six roots or eigenvalues of Σ:

$$\beta^6 - I_1\beta^5 + I_2\beta^4 - I_3\beta^3 + I_4\beta^2 - I_5\beta + I_6 = 0, \tag{17}$$

where

$$I_1 = \sigma_1^2 + \sigma_2^2 + \sigma_3^2 + \sigma_4^2 + \sigma_5^2 + \sigma_6^2, \tag{18a}$$

$$I_2 = \sigma_3^2\sigma_4^2 + \sigma_3^2\sigma_5^2 + \sigma_4^2\sigma_5^2 + \sigma_3^2\sigma_6^2 + \sigma_4^2\sigma_6^2 + \sigma_5^2\sigma_6^2 + \sigma_2^2\sigma_3^2 + \sigma_2^2\sigma_4^2 + \sigma_2^2\sigma_5^2 + \sigma_2^2\sigma_6^2 + \sigma_1^2\sigma_2^2 + \sigma_1^2\sigma_3^2 + \sigma_1^2\sigma_4^2 + \sigma_1^2\sigma_5^2 + \sigma_1^2\sigma_6^2, \tag{18b}$$

$$I_3 = \sigma_3^2\sigma_4^2\sigma_5^2 + \sigma_3^2\sigma_4^2\sigma_6^2 + \sigma_3^2\sigma_5^2\sigma_6 + \sigma_4^2\sigma_5^2\sigma_6^2 + \sigma_2^2(\sigma_5^2\sigma_6^2 + \sigma_4^2(\sigma_5^2 + \sigma_6^2) + \sigma_3^2(\sigma_4^2 + \sigma_5^2 + \sigma_6^2)) + \sigma_1^2(\sigma_4^2\sigma_5^2 + \sigma_4^2\sigma_6^2 + \sigma_5^2\sigma_6^2 + \sigma_3^2(\sigma_4^2 + \sigma_5^2 + \sigma_6^2) + \sigma_2^2(\sigma_3^2 + \sigma_4^2 + \sigma_5^2 + \sigma_6^2)), \tag{18c}$$

$$I_4 = \sigma_3^2\sigma_4^2\sigma_5^2\sigma_6^2 + \sigma_2^2(\sigma_4^2\sigma_5^2\sigma_6^2 + \sigma_3^2(\sigma_5^2\sigma_6^2 + \sigma_4^2(\sigma_5^2 + \sigma_6^2))) + \sigma_1^2(\sigma_3^2\sigma_4^2\sigma_5^2 + \sigma_3^2\sigma_4^2\sigma_6^2 + \sigma_3^2\sigma_5^2\sigma_6^2 + \sigma_4^2\sigma_5^2\sigma_6^2 + \sigma_2^2(\sigma_5^2\sigma_6^2 + \sigma_4^2(\sigma_5^2 + \sigma_6^2) + \sigma_3^2(\sigma_4^2 + \sigma_5^2 + \sigma_6^2))), \tag{18d}$$

$$I_5 = \sigma_2^2\sigma_3^2\sigma_4^2\sigma_5^2\sigma_6^2 + \sigma_1^2(\sigma_3^2\sigma_4^2\sigma_5^2\sigma_6^2 + \sigma_2^2(\sigma_4^2\sigma_5^2\sigma_6^2 + \sigma_3^2(\sigma_5^2\sigma_6^2 + \sigma_4^2(\sigma_5^2 + \sigma_6^2)))), \tag{18e}$$

$$I_6 = \sigma_1^2\sigma_2^2\sigma_3^2\sigma_4^2\sigma_5^2\sigma_6^2. \tag{18f}$$

The first invariant, I_1, is the Trace of S. The last invariant, I_6, is its Determinant. The other invariants represent different combinations of eigenvalues, which can be thought of as distinct features of a 6-dimensional ellipsoid.

These invariants are independent of the coordinate system in which the components of D and E^k are measured, and are intrinsic features of Σ. These invariants are also independent of the order in which the eigenvalues of Σ are sorted (permutation invariant).

Additional intrinsic features of Σ can also be obtained from the invariants of the eigentensors, E^k themselves, which are also easily obtained from the coefficients of the characteristic equations for each of the E^k.

3.7. Visualizing Angular Features of Σ

Can we visualize features of Σ in 3-dimensions? Clearly, such prospects appear dim if we represent Σ as S, a 2nd-order tensor in a 6-dimensional vector space. Alternatively, we propose reducing the dimensionality of Σ by using its spectral decomposition, and visualize features of its eigentensors, E^k, in a 3-dimensional space.

[8] N.B. It is important to ensure that the routines used to perform the eigen decomposition provide an orthonormal basis, particularly when the eigenvalues are repeating. Currently, *Mathematica*™ produces a basis that is linearly independent, but a subsequent Gram–Schmidt procedure is required to make the eigenvectors mutually orthogonal.

To do this, we first form a scalar contraction of Σ with the unit dyadic tensor, $\hat{r}\hat{r}^{\mathrm{T}}$,

$$\hat{r}\hat{r}^{\mathrm{T}} : \Sigma : \hat{r}\hat{r}^{\mathrm{T}} = (\hat{r} \otimes \hat{r}) : \Sigma : (\hat{r} \otimes \hat{r}), \tag{19}$$

where $\hat{r}$ is a unit direction vector. Eq. (19) represents the projection of the 4th-order tensor along the ray or *orientation* specified by $\hat{r}$ and $-\hat{r}$. Fig. 1(a) shows 3-dimensional plots of such projections for the 4th-order isotropic and identity tensors. As expected, no angular dependence is seen for either one. In Figs. 1(b) and (c), two different cases of a cubic orthotropic tensor are shown with different parameters a, b, and c.[9]

Now, we perform a spectral decomposition of Σ, i.e.,

$$\hat{r}\hat{r}^{\mathrm{T}} : \sigma_k E^k \otimes E^k \sigma_k : \hat{r}\hat{r}^{\mathrm{T}}, \tag{20}$$

and then parameterize $\hat{r}$ using spherical coordinates, θ and ϕ:

$$\hat{r}^{\mathrm{T}}(\theta, \phi) = (\sin\theta\cos\phi,\ \sin\theta\sin\phi,\ \cos\theta). \tag{21}$$

The unit 2nd-order dyadic tensor $\hat{r}\hat{r}^{\mathrm{T}}$ is then given by

$$\begin{pmatrix} \cos^2\phi\sin^2\theta & \cos\phi\sin^2\theta\sin\phi & \cos\theta\cos\phi\sin\theta \\ \cos\phi\sin^2\theta\sin\phi & \sin^2\theta\sin^2\phi & \cos\theta\sin\theta\sin\phi \\ \cos\theta\cos\phi\sin\theta & \cos\theta\sin\theta\sin\phi & \cos^2\theta \end{pmatrix}. \tag{22}$$

It is easy to verify that the tensor in Eq. (22) has Rank = 1, so it is line or ray-like, having a distinct *orientation* but no preferred *direction*. Eq. (20) can be further simplified using a few lines of algebra:

$$\hat{r}\hat{r}^{\mathrm{T}} : \sigma_k E^k \otimes E^k \sigma_k : \hat{r}\hat{r}^{\mathrm{T}} = \sum_{k=1}^{6} (\sigma_k \hat{r}^{\mathrm{T}} E^k \hat{r})^2. \tag{23}$$

The term $\hat{r}^{\mathrm{T}} E^k \hat{r}$ above represents the projection of E^k, along $\hat{r}$. Eq. (23) shows the angular structure of Σ as the weighted sum of the projections of these six eigentensors.

Moreover, each eigentensor, E^k, can be further decomposed into a sum of its three eigenvalues, γ_i^k, and three corresponding eigenvectors , v_i^k:

$$\begin{aligned} \sum_{k=1}^{6} (\sigma_k \hat{r}^{\mathrm{T}} E^k \hat{r})^2 &= \sum_{k=1}^{6} \left(\sum_{i=1}^{3} \sigma_k \hat{r}^{\mathrm{T}} \gamma_i^k v_i^k v_i^{k\mathrm{T}} \hat{r} \right)^2 \\ &= \sum_{k=1}^{6} \left(\sum_{i=1}^{3} \sigma_k \gamma_i^k (\hat{r} \cdot v_i^k)^2 \right)^2. \end{aligned} \tag{24}$$

[9]Since all of the eigenvalues are positive, all of the "blobs" depicted in these figures represent positive contributions.

To understand the meaning of Eq. (24), consider the contribution to the sum solely due to eigentensor E^4, given in Eq. (15b). E^4 has three eigenvalues: $\gamma_1^4 = 1$, $\gamma_2^4 = -1$, $\gamma_3^4 = 0$; and three corresponding orthogonal eigenvectors: $v_1^4 = 1/\sqrt{2}\{1, 1, 0\}^{\mathrm{T}}$, $v_2^4 = 1/\sqrt{2}\{1, -1, 0\}^{\mathrm{T}}$, $v_3^4 = \{0, 0, 1\}^{\mathrm{T}}$. Thus, E^4 is a 2nd-order tensor whose Range lies in the x–y plane and whose Kernel (or Null Space) lies along the z-axis. Substituting the eigenvalues above into the 4th term of the sum in Eq. (24) for E^4, we obtain,

$$\begin{aligned} \sum_{i=1}^{3} (\sigma_4 \gamma_i^4 (\hat{r} \cdot v_i^4)^2)^2 &= \sigma_4^2 (\gamma_1^4 (\hat{r} \cdot v_1^4)^2 + \gamma_2^4 (\hat{r} \cdot v_2^4)^2 \\ &\quad + \gamma_3^4 (\hat{r} \cdot v_3^4)^2)^2 = \sigma_4^2 ((\hat{r} \cdot v_1^4)^2 - (\hat{r} \cdot v_2^4)^2)^2. \end{aligned} \tag{25}$$

Therefore, when $\hat{r}$ lies within the x–y plane, and is oriented parallel or anti-parallel to eigenvectors v_1^4 or v_2^4, there will be a positive contribution in Eq. (25) proportional to σ_4^2, otherwise its contribution will be close to zero. Also, if $\hat{r}$ is oriented along or near the z-axis, the sum in Eq. (25) will also be close to zero. The graphical representation of the squared projection of E^4 along $\hat{r}$ (in Eq. (25)) will consist of a quatrefoil-shaped pancake that lies predominantly in the x–y plane, whose lobes are symmetrically oriented along the lines $y = \pm x$. Fig. 2a depicts this object.

We can perform a similar algebraic and graphical analysis of the contributions from all six eigentensors of Σ. Fig. 2a shows the individual and composite 3-dimensional representations of the outer product of each eigentensor, $E^k \otimes E^k$, contracted with $\hat{r}\hat{r}^{\mathrm{T}}$. In general, when the orientation of $\hat{r}$ and one of the eigenvectors of E^k closely overlap then there will be a contribution in the sum in Eq. (24), which will be weighted by the product of the square of the eigenvalues of Σ and of E^k, $(\sigma_k \gamma_i^k)^2$. Otherwise, the contribution will be negligibly small. Figs. 2b and 2c show the angular structure of the 4th-order identity and cubic orthotropic tensors.

This simple interpretation of the contraction of $\hat{r}\hat{r}^{\mathrm{T}}$ and Σ also provides insight into the action of a 2nd-order full Rank tensor (i.e., Rank 3) on Σ or Σ^{-1}, specifically, in the expression appearing in the exponent of Eq. (2):

$$\begin{aligned} &(D - \bar{D}) : \Sigma^{-1} : (D - \bar{D}) \\ &\quad = (D - \bar{D}) : \sigma_k^{-1} E^k \otimes E^k \sigma_k^{-1} : (D - \bar{D}). \end{aligned} \tag{26}$$

We can now expand $D - \bar{D}$ spectrally in terms of its three eigenvalues, λ_i, and three corresponding orthogonal eigenvectors, η_i, (as in [32]) i.e.,

$$D - \overline{D} = \lambda_i \eta_i \eta_i^T. \tag{27}$$

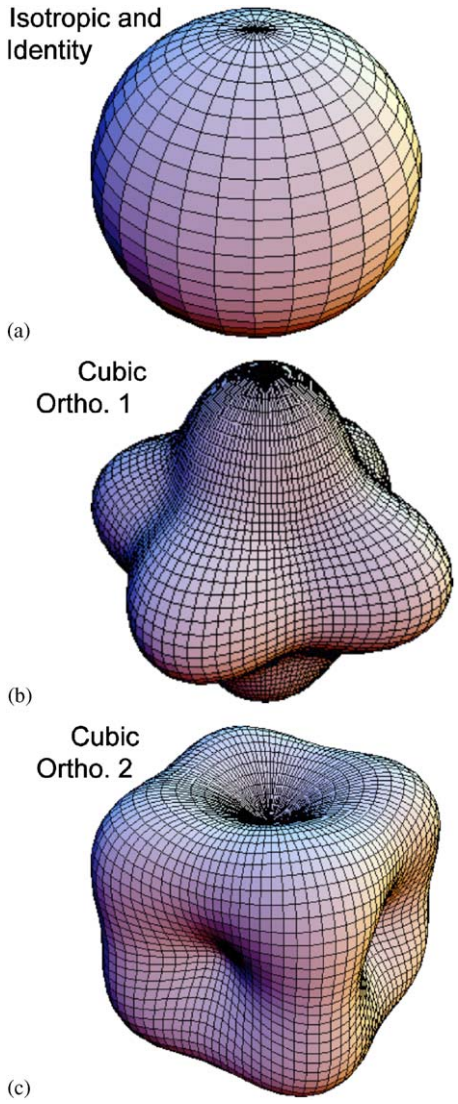

Fig. 1. Radial or angular projection of various 4th-order tensors, Σ, using Eq. (19) or Eq. (23) for (a) both isotropic and unit tensors, and (b) and (c) two different 4th-order cubic tensors. All isotropic tensors (including the identity tensor) exhibit a spherical profile for all admissible values of the parameters χ_κ and χ_μ. For cubic orthotropy, projections are obtained using cubic 4th-order covariance tensors with parameters (b) $a = 80$, $b = 100$, $c = 50\,\mathrm{mm}^4/\mathrm{s}^2$ and (c) $a = 300$, $b = 50$, $c = 40\,\mathrm{mm}^4/\mathrm{s}^2$.

This produces an expression similar to Eq. (24):

$$(D-\bar{D}) : \sigma_k^{-1} E^k \otimes E^k \sigma_k^{-1} : (D-\bar{D}) = \sum_{k=1}^{6} \left(\sum_{i=1}^{3} \frac{\lambda_i}{\sigma_k} \eta_i^{\mathrm{T}} E^k \eta_i \right)^2 = \sum_{k=1}^{6} \left(\sum_{i,j=1}^{3} \frac{\lambda_i \gamma_j^k}{\sigma_k} \eta_i^{\mathrm{T}} v_j^k v_j^{k\mathrm{T}} \eta_i \right)^2, \tag{28}$$

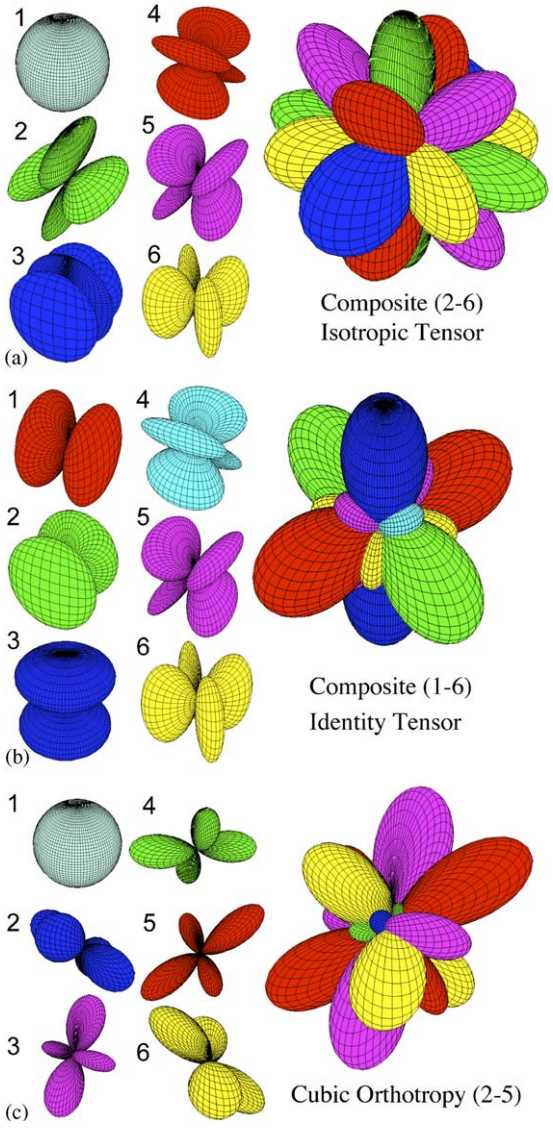

Fig. 2. Visualization of the radial projections of the six orthogonal eigentensors of various 4th-order tensors plotted using Eq. (23) (left) along with the "composite" 4th-order covariance tensor plotted (right). Different colors are used to depict the different 2nd-order eigentensors or eigenmodes. Shown are (a) isotropic (Σ^{iso}), (b) unit, Y, and (c) cubic tensors. In (a) and (c), the sphere associated with the isotropic eigentensor E^1 is not shown since it dominates the angular dependence.

which can be further simplified:

$$(D-\bar{D}) : \sigma_k^{-1} E^k \otimes E^k \sigma_k^{-1} : (D-\bar{D}) = \sum_{k=1}^{6} \left(\sum_{i,j=1}^{3} \frac{\lambda_i \gamma_j^k}{\sigma_k} (\eta_i \cdot v_j^k)^2 \right)^2. \tag{29}$$

The term in parenthesis on the right-hand side of Eq. (29) measures the statistical coherence or

similarity between $D-\bar{D}$ and the various eigentensors, E^k. This coherence is determined by the relative size of the eigenvalues, $(\lambda_i\gamma_j^k/\sigma_k)$, and the degree of collinearity of their corresponding normalized eigenvectors, $(\eta_i \cdot v_j^k)^2$.

Clearly, the qualitative and quantitative analyses performed above would not be feasible using the conventional multi-variate normal distribution in Eq. (1) in which the 6×6 matrix, S, describes the uncertainty associated with a 2nd-order normal tensor random variable that is represented as a vector. Our analysis is also made possible by viewing both the random variable and the parameters appearing in the distribution as tensors, and by employing the spectral decomposition of Σ.

3.8. Expected value of the mean and variance of the ADC, $\hat{r}^{\mathrm{T}}D\hat{r}$

Frequently, it is useful to obtain estimates of projections of D along a particular direction, $\hat{r}$, i.e., $\hat{r}^{\mathrm{T}}D\hat{r}$. For example, in DTI, this scalar quantity represents the ADC that one measures along directions $\hat{r}$ or $-\hat{r}$. Thus, it is important to know the expected value of the first and second moments of $\hat{r}^{\mathrm{T}}D\hat{r}$ [33].

The expected value of $\hat{r}^{\mathrm{T}}D\hat{r}$ is given by

$$E(\hat{r}^{\mathrm{T}}D\hat{r}) = \hat{r}^{\mathrm{T}}E(D)\hat{r} = \hat{r}^{\mathrm{T}}\bar{D}\hat{r}. \tag{30}$$

Therefore, the mean ADC along direction $\hat{r}$ is just the projection of the mean tensor, $\bar{D}$ along $\hat{r}$. In DTI, the angular distribution of $\hat{r}^{\mathrm{T}}\bar{D}\hat{r}$ is often plotted in 3-dimensions, exhibiting a profile that can be "peanut" or "discoid" shaped in brain white matter [34,35].

The variance of the ADC indicates the thickness of the cloud of uncertainty (or "peach fuzz") surrounding the mean "peanut", "discoid" or "sphere" calculated above in Eq. (30). The expected value of the variance of this ADC is given by

$$\begin{aligned} Var(\hat{r}^{\mathrm{T}}D\hat{r}) &= E((\hat{r}^{\mathrm{T}}D\hat{r} - E(\hat{r}^{\mathrm{T}}D\hat{r}))^2) \\ &= E((\hat{r}^{\mathrm{T}}D\hat{r} - \hat{r}^{\mathrm{T}}\bar{D}\hat{r})^2), \end{aligned} \tag{31}$$

which can be written as:

$$Var(\hat{r}^{\mathrm{T}}D\hat{r}) = \hat{r}^{\mathrm{T}}E((D-\bar{D})\hat{r}\hat{r}^{\mathrm{T}}(D-\bar{D}))\hat{r}. \tag{32}$$

Thus, the variance of the ADC measured along the direction, $\hat{r}$, is not simply the projection of a 2nd-order covariance matrix, $E(D^2)-\bar{D}^2$, along $\hat{r}$; it also depends on $\hat{r}^{\mathrm{T}}\hat{r}$. It is not clear how to evaluate the expression in Eq. (32) using standard multi-variate statistical methods. However, using the 4th-order covariance tensor framework developed above, we can rewrite this equation in an equivalent form:

$$Var(\hat{r}^{\mathrm{T}}D\hat{r}) = \hat{r}\hat{r}^{\mathrm{T}}E((D-\bar{D})\otimes(D-\bar{D}))\hat{r}\hat{r}^{\mathrm{T}}. \tag{33}$$

We now recognize the term in parenthesis above in Eq. (33) as the expected value of Σ (see Eq. (A.3) below). Therefore, we obtain the same expression for the variance of the ADC that we did in Eq. (19):

$$Var(\hat{r}^{\mathrm{T}}D\hat{r}) = \hat{r}\hat{r}^{\mathrm{T}} : \Sigma : \hat{r}\hat{r}^{\mathrm{T}}. \tag{34}$$

So, the variance of the ADC along $\hat{r}$ equals the projection of the 4th-order covariance tensor, Σ, along $\hat{r}^{\mathrm{T}}\hat{r}$. This is the first closed-form expression for $Var(ADC)$ as a function of orientation that we are aware of.

Fig. 3 shows a way to visualize the orientational structure of the variance of the ADC. It shows a cut-away of a diffusion "discoid" obtained from Eq. (30) in a hypothetical brain white matter region along with two additional bounding surfaces depicting one standard deviation greater and smaller than the mean. The standard deviation is obtained by taking the square root of Eq. (34).

3.9. Applications to directional statistics

Eq. (19) above also suggests a possible angular distribution for directional data, which does not appear to have been proposed previously. One could construct a Gaussian distribution for the unit dyadic $\hat{r}\hat{r}^{\mathrm{T}}$ of the form

$$p(\hat{r}\hat{r}^{\mathrm{T}}(\theta,\phi)) = \mathrm{e}^{-(1/2)(\hat{r}\hat{r}^{\mathrm{T}}-\overline{\hat{r}\hat{r}^{\mathrm{T}}}):\Sigma_d^{-1}:(\hat{r}\hat{r}^{\mathrm{T}}-\overline{\hat{r}\hat{r}^{\mathrm{T}}})} \Big/ \int_0^{2\pi}\int_0^{\pi} \mathrm{e}^{-(1/2)(\hat{r}\hat{r}^{\mathrm{T}}-\overline{\hat{r}\hat{r}^{\mathrm{T}}}):\Sigma_d^{-1}:(\hat{r}\hat{r}^{\mathrm{T}}-\overline{\hat{r}\hat{r}^{\mathrm{T}}})} \sin\theta\,\mathrm{d}\theta\,\mathrm{d}\phi, \tag{35}$$

where $\hat{r}^{\mathrm{T}}$ is again parameterized by θ and ϕ as above in Eqs. (21) and (22). This distribution has a mean dyadic, $\overline{\hat{r}\hat{r}^{\mathrm{T}}}$, and a general 4th-order covariance tensor, Σ_d, both of which admit many types of angular distributions (e.g., polar, girdle). A more compact representation of the distribution in Eq. (35) can be obtained by using the result in Eq. (23):

$$p(\hat{r}\hat{r}^{\mathrm{T}}(\theta,\phi)) = \frac{\mathrm{e}^{-(1/2)\sum_{k=1}^{6}(\sigma_k^{-1}(\hat{r}-\bar{\hat{r}})^{\mathrm{T}}E_d^k(\hat{r}-\bar{\hat{r}}))^2}}{\int_0^{2\pi}\int_0^{\pi}\mathrm{e}^{-(1/2)\sum_{k=1}^{6}(\sigma_k^{-1}(\hat{r}-\bar{\hat{r}})^{\mathrm{T}}E_d^k(\hat{r}-\bar{\hat{r}}))^2}\sin\theta\,\mathrm{d}\theta\,\mathrm{d}\phi}. \tag{36}$$

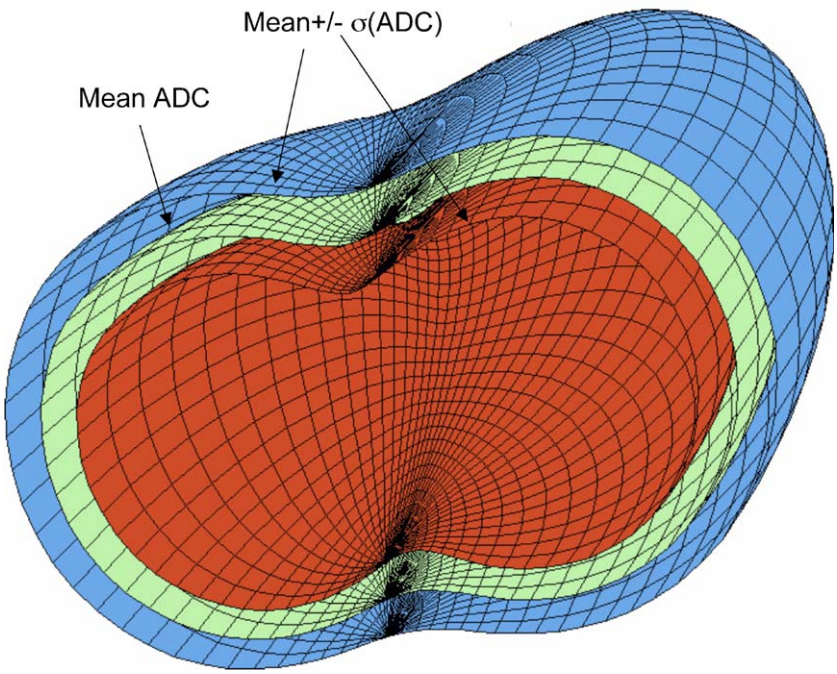

Fig. 3. Three-dimensional angular dependence of the mean ADC, $\hat{r}^{\mathrm{T}}\bar{D}\hat{r}$, bounded by its standard deviation (std.dev.). The middle isosurface (Green) corresponds to the mean ADC, and the two bounding surfaces are placed at the mean $ADC+\sigma_{ADC}$ (Blue) and the mean $ADC-\sigma_{ADC}$ (Red). The mean ADC and σ_{ADC} are obtained using Eqs. (30) and (34).

A study of the properties of this distribution will hopefully be the subject of future work.

4. Results

We introduce noise into diffusion tensor data using Monte Carlo methods (as in [36]), in which normally distributed white noise is added to both the real and imaginary channels of the MR signal obtained from a diffusion weighted MR sequence. The resulting magnitude diffusion weighted signals are distributed according to the Rician distribution [37]. Such measurements are made with diffusion gradient vectors applied along at least six non-collinear and non-coplanar directions. Non-diffusion weighted signals are also obtained. From this data, we can estimate the diffusion tensor using linear or non-linear regression [10]. How many diffusion gradient directions to use and how to orient them to obtain an optimally designed DTI experiment are active areas of research [38–41].

Using the tensor-variate normal distribution in Eq. (2), we previously argued that an optimal experimental design should produce an isotropic 4th-order covariance tensor [17], as in Eq. (14), or a close approximation to it. If the models in DTI were linear, the simplest scheme that produces an isotropic 4th-order covariance tensor is a scheme in which the diffusion gradient vectors form the vertices of an icosahedron. When the six non-collinear vertices are also pair-wise antipodally symmetric, we call it an icosahedral acquisition scheme. In our simulations, we use an icosahedral scheme with four repetitions, meaning that four measurements are made along each gradient direction in addition to 4 non-diffusion weighted images. From these 28 measurements, we estimate a diffusion tensor.

Although, different experimental designs and different paradigmatic tissue types found in human brain were used in our simulations, we show here only results obtained using the icosahedral acquisition scheme and two different tissue types: one with isotropic diffusion properties (characteristic of gray matter) with all principal diffusivities equal to $700\,\mathrm{mm}^2/\mathrm{s}$, and another with anisotropic diffusion properties (characteristic of white matter), with principal diffusivities equal to 1000, 700, and $400\,\mathrm{mm}^2/\mathrm{s}$. In each case, we obtained 1000 diffusion tensor replicates from which the sample 4th-order covariance tensor is estimated directly using Eq. (A.14), except that we replace the factor of "N" appearing in the denominator with "$N-1$". We then

perform a spectral decomposition of the 4th-order sample covariance tensors. The projections of the eigentensor components are shown for the isotropic diffusion case in Fig. (4a) and for the anisotropic diffusion case in Fig. (4b). The former case results in a 4th-order covariance tensor whose pattern of degeneracy more closely resembles the isotropic 4th-order tensor with eigenvalues {89.1, 50.6, 50.1, 49.5, 41.1, 37.8} mm^4/s^2 than the latter, with eigenvalues {81.5, 54.5, 49.6, 44.5, 23.0, 16.8} mm^4/s^2.

5. Discussion

One is often interested in determining the statistical properties of 2nd-order tensor *fields*, which are measured or sampled discretely within a spatial domain or imaging volume. To do this, we must distinguish between the different types of variability in tensor data. Sampled tensor data can vary within a particular voxel in an imaging volume solely because of background MR noise. Also, the mean and covariance tensors can themselves vary with position within the imaging volume since tensor fields can be heterogeneous (i.e., with the mean tensor explicitly varying with position) and/or anisotropic (i.e., exhibiting directional bias in the mean tensor) as is clearly demonstrated in [42].

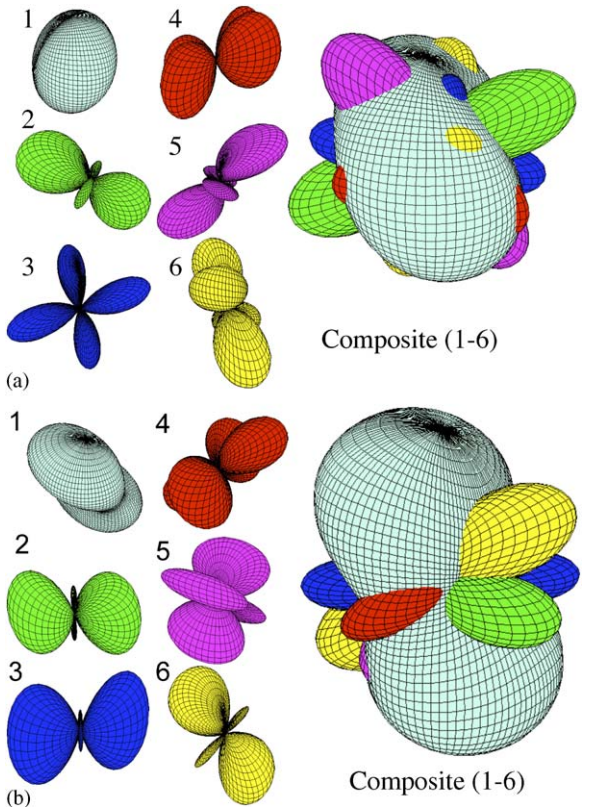

Fig. 4. Sample 4th-order covariance tensors obtained using Monte Carlo simulations of DTI experiments. An icosahedral gradient sampling scheme described in [17] is used with four repetitions and four non-diffusion weighted images, $S/N = 20$. Isotropic diffusion tensors are used with mean diffusivity = 700 mm^2/s; anisotropic diffusion tensors are drawn with principal diffusivities: 1000, 700, 400 mm^2/s. Projections of the individual eigentensors of the sample 4th-order covariance tensor for the isotropic diffusion case is shown in (a) as six individual eigentensor projections along with a composite tensor. Similarly, the spectral components of the sample 4th-order covariance tensor are shown in (b) for the anisotropic diffusion case.

Naïvely, one could treat the problem of characterizing noisy, heterogeneous, anisotropic tensor fields by determining a joint probability distribution, $p(D_1, D_2, D_3, \ldots, D_N)$, of 2nd-order tensors, $D_1,\ldots,D_N$, sampled at different points throughout the imaging volume or domain. These tensors are assumed to be correlated because of the spatial structure inherent in either continuous or piece-wise continuous tensor fields. This approach, unfortunately, is inefficient, leading to a proliferation of free parameters without providing information about the spatial variability of the statistical parameters of the underlying tensor field.

If we are assured that the tensor field is everywhere described by the normal tensor-variate distribution, then a more pragmatic approach is to characterize noise, heterogeneity and anisotropy together using Eq. (2) with the mean and covariance tensors of this distribution given explicitly as functions of the position vector, $\mathbf{r}$, within the imaging volume (or spatial domain), i.e.:

$$p(D(\mathbf{r})) = \sqrt{\frac{|\Sigma^{-1}|}{8\pi^6}}\, e^{-(1/2)(D(\mathbf{r})-\tilde{D}(\mathbf{r})):\Sigma^{-1}(\mathbf{r}):(D(\mathbf{r})-\tilde{D}(\mathbf{r}))} = \sqrt{\frac{|\Sigma^{-1}|}{8\pi^6}}\, e^{-(1/2)(D_{ij}(\mathbf{r})-\tilde{D}_{ij}(\mathbf{r})):\Sigma^{-1}_{ijmn}(\mathbf{r}):(D_{mn}(\mathbf{r})-\tilde{D}_{mn}(\mathbf{r}))}. \quad (37)$$

Above, $p(D(\mathbf{r}))$ represents the pdf of $D(\mathbf{r})$.

In applications, such as DTI of the brain, diffusion properties are generally continuous on a macroscopic length scale except at tissue boundaries (for instance between sub-cortical white matter and cortical gray matter, between cortical gray matter and cerebrospinal fluid (CSF), and between white matter and CSF-filled ventricles in the brain). While in gray matter and CSF-filled regions the diffusion tensor field is approximately homogeneous and

isotropic, in many white matter areas, it is heterogeneous and anisotropic [43].

Even so, it is our goal to find a piece-wise continuous approximation to $\bar{D}(\mathbf{r})$ and $\Sigma(\mathbf{r})$ within the imaging volume [46]. This information would be useful in segmenting gray matter, white matter, and CSF in DTI brain data to facilitate comparisons among different brain regions within the same subject and among multiple subjects based on differences in their statistical properties.

Within certain domains, e.g., along white matter fascicles or nerve bundles, in which the underlying $\bar{D}(\mathbf{r})$ and $\Sigma(\mathbf{r})$ tensor fields are assumed continuous, it may be possible to obtain a piece-wise continuous approximation to the three individual eigenvalue and eigenvector fields of $\bar{D}(\mathbf{r})$ and the six individual eigenvalue and eigentensor fields of $\Sigma(\mathbf{r})$, i.e.,

$$\bar{D}(\mathbf{r}) = \lambda_i(\mathbf{r})\eta_i(\mathbf{r})\eta_i^{\mathrm{T}}(\mathbf{r});$$
$$\Sigma(\mathbf{r}) = \sigma_k(\mathbf{r})E^k(\mathbf{r}) \otimes E^k(\mathbf{r})\sigma_k(\mathbf{r}). \quad (38)$$

This information could enable us to classify or segment different tissue types according to their underlying symmetries (multiplicities of eigenvalues) and properties of their eigentensors (e.g., Rank, mode type). While similar classification schema are employed in applied mechanics [14,27], we are not aware that this has been done in statistical applications.

In fact, methods to obtain a continuous approximation to $\bar{D}(\mathbf{r})$ have already been developed [42,44]. The theoretical framework presented in [45] and subsequently implemented in [42] can be extended to obtaining continuous approximations to 4th-order and higher order tensor fields.

An interesting issue arises when one obtains a continuous approximation for a discrete, sampled tensor field, $\bar{D}(\mathbf{r}_n)$, that is presumed to be positive definite. It has been proposed that interpolating or approximating sampled tensor data should be performed within a manifold of positive definite tensors (i.e., a "symmetric space") [47], a notion recently promulgated by Batchelor and colleagues (see [48,49]) and further elaborated upon by groups at INRIA [50,51]. The positive definiteness constraint, however, is not used above to derive the form of the normal tensor-variate distribution given in Eq. (2), nor was it imposed previously to determine a continuous approximation to the diffusion tensor field given in [42]. Future work will focus on establishing the exact relationship between the Riemannian (or symmetric space) representation and the Euclidean space representation of the tensor-variate distribution, and determining what errors, if any, might be introduced when one obtains an approximation to these tensor fields on a Euclidean rather than a Riemannian manifold. One would expect that when the mean tensor is positive definite and the covariance tensor is sufficiently "compact" (so that the majority of 2nd-order random tensors generated by such a distribution are still predominantly positive definite), the tensor manifold will be locally "flat", and the normal tensor-variate distribution should suffice. This is likely to be the situation in most current DTI applications in which the signal-to-noise ratio (SNR) of the diffusion weighted image data is sufficiently high ($>20/1$) and the measured mean diffusion tensor components are sufficiently large that the overwhelming majority of estimated diffusion tensors are positive definite without the need to impose a positive-definiteness constraint explicitly when estimating them statistically.

Because of known physical constraints and additional *a priori* information, it is sometimes possible to establish bounds or limits on the coefficients of the 4th-order tensor describing the properties of elastic media when developing continuum mechanical models of materials, in addition to those imposed by the various material symmetries described above. In materials engineering and continuum mechanics, much has been written about establishing bounds on the 4th-order elasticity tensor [52] using *a priori* information about the physical system under study. It is reasonable to propose that constraints and other *a priori* information could also restrict the form of Σ in the context of applying Eq. (2) above, and in particular, developing models of covariance. This appears to be a rich area for further inquiry.

This new statistical methodology could be applied in various disciplines. In imaging sciences and signal processing, the most obvious uses are in feature detection, pattern classification, and segmentation of diffusion tensor MRI data, and for a variety of clinical, biological, and materials sciences applications. In physics, chemistry, applied physics, and materials sciences, quantities such as the moment of inertia tensors, rotational diffusion tensors, and elastic coefficient tensors (e.g., of elastic media, nematics, crystals) [53] are routinely measured, as well as permittivity and permeability tensors. In continuum mechanics and materials engineering applications, tensor quantities are ubiquitous in

constitutive equations that describe charge, mass, momentum, and energy transport. These include the Reynolds' stress tensor, the translational diffusion tensor, the particle dispersion tensor, the fabric tensor, the electrical conductivity tensor, the heat conductivity tensor, the thermal expansion tensor, and the hydraulic permeability tensor [54]. In hydrodynamics, oceanography, and meteorology, velocity fields are routinely sampled from which shear-rate tensors can be estimated and analyzed using these approaches. Finally, in geophysics, the magnetic susceptibility tensor is often measured and analyzed from core samples [55,56].

In the potential applications listed above, one may be presented with data in which a 2nd-order tensor or a discrete, noisy tensor field is measured. To characterize features of the governing statistical distribution, particularly the 2nd-order mean and 4th-order covariance tensors, we could now adopt and use a schema similar to that described in Dellinger et al. [28], originally proposed to classify anisotropic solids. We could establish a hierarchy of possible covariance models (or forms) based on the various symmetries exhibited by the 4th-order covariance tensor (e.g., isotropy, transverse isotropy). As discussed in [28] and in Helbig [57], the pattern of the eigenvalues could be used to determine the type of symmetry exhibited by the 4th-order covariance tensor. A 6-fold degeneracy {A, A, A, A, A, A} indicates the identity tensor (with a scale factor A); the pattern {A, B, B, B, B, B} indicates an isotropic tensor; {A, B, B, C, C, C} indicates cubic orthotropy; {A, B, C, C, D, D} indicates transverse isotropy, etc. When the experiment is noisy, of course, this degeneracy will only be approximate, so determining the underlying type of symmetry must be performed statistically, at a prescribed confidence level. Using this idea, one can try to obtain the most parsimonious description of Σ, i.e., the model of statistical anisotropy that provides the best fit to the experimental data using the fewest free parameters. This approach would allow us to represent the dependencies among tensor variables using a small number of free parameters, and classify the type of statistical anisotropy observed in tensor measurements.

6. Concluding remarks

We have seen that preserving the algebraic form of a 2nd-order random tensor, D, and its related statistical parameters (i.e., its 2nd-order mean and 4th-order covariance tensors, $\bar{D}$ and Σ) leads naturally to considering the properties and eigenstructure of Σ. In particular, in generalizing the spectral decomposition from matrices or 2nd-order tensors to Σ, we obtain new and useful features with which to represent and visualize 2nd-order tensor data, and a hierarchy of possible symmetries with which to classify them. These properties and features would be difficult, if not impossible, to glean if we treated 2nd-order tensor random variables as vector-valued random variables, as is the convention in multi-variate statistical analysis.

Acknowledgments

We gratefully acknowledge Liz Salak for editing this document. We would also like to thank Evren Özarslan for providing many insightful suggestions, and Albert Tarantola for clarifying many useful properties of 4th-order tensors. This research was supported by the Intramural Research Program of NICHD.

Appendix A

Expectations of moments of tensor random variables

The expected value of the 2nd-order random tensor is given by

$$E(D) = \bar{D}. \tag{A.1}$$

For the normal tensor-variate distribution, this quantity would be computed as follows:

$$E(D) = \sqrt{\frac{|\Sigma^{-1}|}{8\pi^6}} \iiiiiint D \, \mathrm{e}^{-\frac{1}{2}(D-\bar{D}):\Sigma^{-1}:(D-\bar{D})} \, \mathrm{d}D. \tag{A.2}$$

The maximum likelihood estimate of $\bar{D}$ will be discussed below.

The expected value of the 4th-order covariance tensor is:

$$E((D-\bar{D}) \otimes (D-\bar{D})) = E(D \otimes D - D \otimes \bar{D} - \bar{D} \otimes D + \bar{D} \otimes \bar{D}), \tag{A.3}$$

which simplifies to

$$= E(D \otimes D) - (\bar{D} \otimes \bar{D}). \tag{A.4}$$

This would be computed in the following way from the tensor-variate distribution:

$$E(\Sigma) = \sqrt{\frac{|\Sigma^{-1}|}{8\pi^6}} \iiiint\!\!\iint ((D-\bar{D}) \otimes (D-\bar{D}))\, \mathrm{e}^{-\frac{1}{2}(D-\bar{D}):\Sigma^{-1}:(D-\bar{D})}\, \mathrm{d}D, \tag{A.5}$$

which simplifies to

$$E(\Sigma) = \sqrt{\frac{|\Sigma^{-1}|}{8\pi^6}} \iiiint\!\!\iint D \otimes D \mathrm{e}^{-\frac{1}{2}(D-\bar{D}):\Sigma^{-1}:(D-\bar{D})}\, \mathrm{d}D - \bar{D} \otimes \bar{D}. \tag{A.6}$$

Maximum likelihood estimates of moments of a normal tensor random variable

The method for obtaining population estimates of the sample mean and covariance tensors associated with a 2nd-order tensor random variable is analogous to that for a multi-variate distribution. If we assume an experiment in which there are N independent, identically distributed (IID), 2nd-order normal random tensors, D, with mean tensor, $\bar{D}$, and covariance tensor, Σ, then the log-likelihood function for the nth trial, L_n, is given by

$$L_n = -\ln(p(D^n)) = -\ln\left(\sqrt{\frac{|\Sigma^{-1}|}{8\pi^6}}\right) + \frac{1}{2}(D^n-\bar{D}):\Sigma^{-1}:(D^n-\bar{D}). \tag{A.7}$$

Thus, for an experiment with N trials, the log-likelihood function is given by

$$L_N = -\ln\left(\prod_{n=1}^{N} p(D^n)\right) = -N\ln\left(\sqrt{\frac{|\Sigma^{-1}|}{8\pi^6}}\right) + \frac{1}{2}\sum_{n=1}^{N}(D^n-\bar{D}):\Sigma^{-1}:(D^n-\bar{D}). \tag{A.8}$$

The maximum likelihood estimate for the population mean tensor, $\bar{D}$, is given by the condition

$$\frac{\partial L_N}{\partial \bar{D}} = \frac{\partial}{\partial \bar{D}} \sum_{n=1}^{N}(D^n-\bar{D}):\Sigma^{-1}:(D^n-\bar{D}) = 0. \tag{A.9}$$

This simplifies to

$$\sum_{n=1}^{N} \Sigma^{-1}:(D^n-\bar{D}) = \Sigma^{-1}:\sum_{n=1}^{N}(D^n-\bar{D}) = 0, \tag{A.10}$$

which is satisfied for all admissible Σ^{-1} only when

$$\sum_{n=1}^{N}(D^n-\bar{D}) = 0. \tag{A.11}$$

This leads to

$$\bar{D} = \frac{1}{N}\sum_{n=1}^{N} D^n \quad \text{or} \quad \bar{D}_{ij} = \frac{1}{N}\sum_{n=1}^{N} D^n_{ij}, \tag{A.12}$$

which simply states that the arithmetic mean of the sampled D data is the maximum likelihood estimate of the population mean tensor, $\bar{D}$.

The maximum likelihood estimate of the population covariance tensor, Σ, can be obtained from

$$\frac{\partial L_N}{\partial \Sigma^{-1}} = 0. \tag{A.13}$$

Following a derivation similar to that used for multi-variate distributions, e.g., see [19], we obtain

$$\Sigma = \frac{1}{N}\sum_{m=1}^{N}(D^m-\bar{D}) \otimes (D^m-\bar{D}) \text{ or}$$

$$\Sigma_{ijkl} = \frac{1}{N}\sum_{m=1}^{N}(D^m_{ij}-\bar{D}_{ij})(D^m_{kl}-\bar{D}_{kl}). \tag{A.14}$$

Although Σ^{-1} must be obtained to specify the normal distribution for D, it is not required to expand the sample 4th-order covariance tensor using the generalized spectral decomposition. However, Σ^{-1} is readily computed by converting Σ into an equivalent 6-dimensional inverse covariance tensor, S, inverting it, and then reassigning the elements of S^{-1} to those of Σ^{-1}.

References

[1] K. Pearson, On lines and planes of closest fit to systems of points in space, Philos. Mag. 6 (2) (1901) 559–572.

[2] H. Hotelling, Analysis of a complex of statistical variables into principal components, J. Educ. Psychol. 24 (1933) 417–444 and 498–520.

[3] C. Spearman, The proof and measurement of association between two things, Am. J. Psychol. 15 (1933) 72 and 202.

[4] S. Makeig, T.P. Jung, A.J. Bell, D. Ghahremani, T.J. Sejnowski, Blind separation of auditory event-related brain responses into independent components, Proc. Natl. Acad. Sci. USA 94 (20) (1997) 10979–10984.

[5] A.J. Bell, T.J. Sejnowski, The "independent components" of natural scenes are edge filters, Vision Res. 37 (23) (1997) 3327–3338.

[6] J. Herault, C. Jutten, Blind separation of sources, part 1: an adaptive algorithm based on neuromimetic architecture, Signal Process. 24 (1991) 1–10.

[7] A. Bell, T. Sejnowski, An information-maximization approach to blind separation and blind deconvolution, Neural Comput. 7 (6) (1995) 1129–1159.
[8] J. Ruiz-Alzola, C.-F. Westin, Tensor signal processing, Signal Process. 84 (2004) 2461–2463.
[9] P.J. Basser, J. Mattiello, D. Le Bihan, MR diffusion tensor spectroscopy and imaging, Biophys. J. 66 (1) (1994) 259–267.
[10] P.J. Basser, J. Mattiello, D. Le Bihan, Estimation of the effective self-diffusion tensor from the NMR spin echo, J. Magn. Reson. B 103 (3) (1994) 247–254.
[11] K. Fukunaga, Introduction to statistical pattern recognition, in: H.G. Booker, N. DeClaris (Eds.), Electrical Sciences, Academic Press Inc., New York, 1972.
[12] J. Betten, W. Helisch, Irreduzible Invarianten eines Tensors vierter Stufe, (ZAMM) Z. Angew. Math. Mech. 72 (1) (1992) 45–57.
[13] E.T. Onat, J.P. Boehler, J.A.A. Kirillov, On the polynomial invariants of the elasticity tensor, J. Elasticity (1994) 97–110.
[14] M.M. Mehrabadi, S.C. Cowin, J. Jaric, 6-Dimensional orthogonal tensor representation of the rotation about an axis in 3 dimensions, Int. J. Solids Struct. 32 (3–4) (1995) 439–449.
[15] S. Pajevic, P.J. Basser, Parametric and non-parametric statistical analysis of DT-MRI data, J. Magn. Reson. 161 (1) (2003) 1–14.
[16] P.J. Basser, S. Pajevic, Dealing with uncertainty in DT-MRI data, Israel J. Chem. 43 (1-2) (2003) 129–144.
[17] P.J. Basser, S. Pajevic, A normal distribution for tensor-valued random variables: applications to diffusion tensor MRI, IEEE Trans. Med. Imaging 22 (7) (2003) 785–794.
[18] K.V. Mardia, J.T. Kent, J.M. Bibby, Multivariate Analysis, Academic Press, New York, 1979, p. 519.
[19] T.W. Anderson, An Introduction to Multivariate Statistics, second ed., Wiley, New York, 1984, p. 675.
[20] P.M. Morse, H. Feschbach, Methods of Theoretical Physics, vol. 1, McGraw-Hill, New York, 1953, p. 997.
[21] H. Jeffreys, Cartesian Tensors, Cambridge University Press, Cambridge, 1931, p. 93.
[22] A.E.H. Love, The Mathematical Theory of Elasticity, fourth ed, Cambridge University Press, Cambridge, 1945, p. 643.
[23] A.E. Green, W. Zerna, Theoretical Elasticity, second ed, Clarendon Press, Oxford, 1954, p. 457.
[24] W. (Lord Kelvin) Thomson, Elements of a mathematical theory of elasticity, Philos. Trans. R. Soc. 166 (1856) 481.
[25] S. Sutcliffe, Spectral decomposition of the elasticity tensor, Trans. ASME 59 (1992) 762–773.
[26] Q.S. Zheng, A note on representation for isotropic functions of 4th-order tensors in 2-dimensional space, Z. Angew. Math. Mech. 74 (8) (1994) 357–359.
[27] S.C. Cowin, M.M. Mehrabadi, On the identification of material symmetry for anisotropic elastic-materials, Q. J. Mech. Appl. Math. 40 (1987) 451–476.
[28] J. Dellinger, D. Vasicek, C. Sondergeld, Kelvin notation for stabilizing elastic-constant inversion, Rev. L'Inst. Français Pétrole 53 (5) (1998).
[29] M.M. Mehrabadi, S.C. Cowin, Eigentensors of linear anisotropic elastic-materials, Q. J. Mech. Appl. Math. 43 (1990) 15–41.
[30] A. Tarantola, Elements for Physics: Quantities, Qualities, and Intrinsic Theories, Springer, Berlin, 2005, p. 279.
[31] W. (Lord Kelvin) Thomson, Elasticity, Encyclopedia Britannica, vol. 7, ninth ed., Adam and Charles Black, London, Edinburgh, 1878, pp. 796–825.
[32] G. Strang, Linear Algebra and Its Applications, third ed, Cambridge Press, Wellesley, 1988.
[33] J. Kärger, H. Pfeifer, W. Heink, Principles and applications of self-diffusion measurements by nuclear magnetic resonance, in: J. Waugh (Ed.), Advances in Magnetic Resonance, vol. 12, Academic Press, New York, 1988, pp. 1–89.
[34] D.S. Tuch, T.G. Reese, M.R. Wiegell, N. Makris, J.W. Belliveau, V.J. Wedeen, High angular resolution diffusion imaging reveals intravoxel white matter fiber heterogeneity, Magn. Reson. Med. 48 (4) (2002) 577–582.
[35] L.R. Frank, Characterization of anisotropy in high angular resolution diffusion-weighted MRI, Magn. Reson. Med. 47 (6) (2002) 1083–1099.
[36] C. Pierpaoli, P.J. Basser, New invariant "lattice" index achieves significant noise reduction in measuring diffusion anisotropy, in: Proceedings of the ISMRM, New York, 1996, p. 1326.
[37] R.M. Henkelman, Measurement of signal intensities in the presence of noise in MR images, Med. Phys. 12 (2) (1985) 232–233.
[38] D.K. Jones, M.A. Horsfield, A. Simmons, Optimal strategies for measuring diffusion in anisotropic systems by magnetic resonance imaging, Magn. Reson. Med. 42 (3) (1999) 515–525.
[39] D.K. Jones, The effect of gradient sampling schemes on measures derived from diffusion tensor MRI: a Monte Carlo study, Magn. Reson. Med. 51 (4) (2004) 807–815.
[40] S. Skare, M. Hedehus, M.E. Moseley, T.Q. Li, Condition number as a measure of noise performance of diffusion tensor data acquisition schemes with MRI, J. Magn. Reson. 147 (2) (2000) 340–352.
[41] S. Skare, T. Li, B. Nordell, M. Ingvar, Noise considerations in the determination of diffusion tensor anisotropy, Magn. Reson. Imaging 18 (6) (2000) 659–669.
[42] S. Pajevic, A. Aldroubi, P.J. Basser, A continuous tensor field approximation of discrete DT-MRI data for extracting microstructural and architectural features of tissue, J. Magn. Reson. 154 (1) (2002) 85–100.
[43] C. Pierpaoli, P. Jezzard, P.J. Basser, A. Barnett, G. Di Chiro, Diffusion tensor MR imaging of the human brain, Radiology 201 (3) (1996) 637–648.
[44] C. Poupon, J.-F. Mangin, V. Frouin, F. Regis, M. Pachot-Clouard, D. Le Bihan, I. Bloch, Regularization of MR diffusion tensor maps for tracking brain white matter bundles, in: Proceedings of MICCAI'98, 1998, pp. 489–498.
[45] A. Aldroubi, P.J. Basser, Reconstruction of vector and tensor fields from sampled discrete data, in: L.W. Baggett, D.R. Larson (Eds.), Contemporary Mathematics, vol. 247, AMS, Providence, RI, 1999, pp. 1–15.
[46] S. Pajevic, A. Aldroubi, P.J. Basser, A continuous tensor field approximation of discrete DT-MRI data, in: D.J. Weickert (Universität des Saarlandes), D. H. Hagen (Universität Kaiserslautern) (Eds.), Visualization and Image Processing of Tensor Fields, Springer Series on Mathematics and Visualization, Springer, Berlin, 2005.
[47] A. Terras, Harmonic Analysis on Symmetric Spaces and Applications II, Springer, Berlin, 1988, p. 385.
[48] P.G. Batchelor, M. Moakher, D. Atkinson, F. Calamante, A. Connelly, A rigorous framework for diffusion tensor calculus, Magn. Reson. Med. 53 (1) (2005) 221–225.

[49] M. Moakher, Means and averaging in the group of rotations, SIAM J. Matrix Anal. Appl. 24 (1) (2002) 1–16.
[50] C. Lenglet, M. Rousson, R. Deriche, O. Faugeras, Statistics on multivariate normal distributions: a geometric approach and its application to diffusion tensor MRI, INRIA, Sophia Antipolis No. 5242, June, 2004.
[51] X. Pennec, Probabilities and statistics on Riemannian manifolds: a geometric approach, INRIA, Sophia Antipolis No. 5093, January, 2004.
[52] M.M. Mehrabadi, S.C. Cowin, C.O. Horgan, Strain-energy density bounds for linear anisotropic elastic-materials, J. Elasticity 30 (2) (1993) 191–196.
[53] L.D. Landau, E.M. Lifshitz, Theory of Elasticity, vol. 7, third ed., Pergamon Press, Oxford, 1986.
[54] J.F. Nye, Physical Properties of Crystals: Their Representation by Tensors and Matrices, Oxford University Press, Oxford, 1985, p. 324.
[55] G.R. Hext, Estimation of second-order tensors with related tests and designs, Biometrika 50 (3–4) (1963) 353–373.
[56] L. Tauxe, N. Kylstra, C. Constable, Bootstrap statistics for paleomagnetic data, J. Geophys. Res.-Solid Earth Planets 96 (B7) (1991) 11723–11740.
[57] K. Helbig, Foundations of Anisotropy for Exploration Seismics, first ed., Elsevier, Oxford, 1994, p. 502.